A Learning Scheme for Microgrid Islanding and Reconnection

Carter Lassetter, *Student Member, IEEE,* Eduardo Cotilla-Sanchez, *Member, IEEE,* and Jinsub Kim, *Member, IEEE*

arXiv:1611.05317v1 [cs.LG] 15 Nov 2016

***Abstract*—This paper introduces a robust learning scheme that can dynamically predict the stability of the reconnection of sub-networks to a main grid. As the future electrical power systems tend towards smarter and greener technology, the deployment of self sufficient networks, or microgrids, becomes more likely. Microgrids may operate on their own or synchronized with the main grid, thus control methods need to take into account islanding and reconnecting said networks. The ability to optimally and safely reconnect a portion of the grid is not well understood and, as of now, limited to raw synchronization between interconnection points. A support vector machine (SVM) leveraging real-time data from phasor measurement units (PMUs) is proposed to predict in real time whether the reconnection of a sub-network to the main grid would lead to stability or instability. A dynamics simulator fed with pre-acquired system parameters is used to create training data for the SVM in various operating states. The classifier was tested on a variety of cases and operating points to ensure diversity. Accuracies of approximately 90% were observed throughout most conditions when making dynamic predictions of a given network.**

***Keywords*—Synchrophasor, machine learning, microgrid, islanding, reconnection**

I. Introduction

As we make strides towards a smarter power system, it is important to explore new techniques and innovations to fully capture the potential of such a dynamic entity. Many large blackout events, such as the blackout of 2003, could have been prevented with smarter controls and better monitoring [1]. Phasor measurement units, or PMUs, are one such breakthrough that will allow progress to be made in both monitoring and implementing control to the system [2]. PMUs allow for direct measurement of bus voltages and angles at high sample rates which makes dynamic state estimation more feasible [3], [4]. With the use of PMUs, it is possible to improve upon current state estimation [5] and potentially open up new ways to control the grid. The addition of control techniques and dynamic monitoring will be important as we begin to integrate newer solutions, such as microgrids, into the power network. With these advanced monitoring devices, microgrids become more feasible due to the potential for real-time monitoring schemes. The integration of microgrids bring many benefits such as the ability to operate while islanded as well as interconnected with the main grid; they provide a smooth integration for renewable energy sources that match local demand. Unfortunately the implementation of microgrids is still challenging due to lacking experience with the behavior of control schemes during off-nominal operation.

Currently, microgrids are being phased in slowly due in part to the difficulty of operating subnetworks independently as well as determining when they can be reconnected to the main grid. Works in the literature have focused on the potential of reconnecting microgrids to the main grid, in particular aiming at synchronizing the buses at points of interconnect with respects to their voltages, frequencies, and angles [6]. Effort has been directed at creating control schemes to minimize power flow at the point of common coupling (PCC) using direct machine control, load shedding, as well as energy storage, to aid in smooth reconnection [7], [8]. Upon reconnection of an islanded sub-network to the main grid, instability can cause damage on both ends. It is important to track instabilities on both the microgrid and main grid upon reconnection to accurately depict the outcome of reconnection. Most works focus on the synchronization of two networks before reconnection [9], [10]. In some cases we may need to look at larger microgrids or subnetworks in which multiple PCCs exist. In such scenarios, it becomes much more difficult to implement a control scheme that satisfies *good* reconnection tolerances in regards to minimizing bus frequency, angle, and voltage differences at each PCC. In addition to the possibility of multiple PCCs, it is possible that direct manipulation of the system becomes limited, compromised, or unsupported with respect to synchronization. In order to address these shortcomings, we implement an algorithm that dynamically tracks and makes predictions based on the system states, providing real-time stability information of potential reconnections.

An algorithm that tracks potential reconnection and islanding times needs to be robust to prevent incorrect operation during these scenarios. PMUs make use of GPS synchronization [11] which can create an attack platform for adversaries by changing or shifting the time synchronization. Incorrect or compromised usage could lead to incorrect predictions that would degrade system stability due to hidden failures that remain dormant until triggered by contingencies [12]. We propose an algorithm that can make accurate predictions in face of potentially compromised measurements.

Due to the complexity of the power grid, it is difficult to come up with a verbatim standard depicting the potential stability after reconnection of a subnetwork. With advances in the artificial intelligence community, we can make use of machine learning algorithms in order to explore vast combinations of sensor inputs, states, and control actions. This can be done in a

C. Lassetter, E. Cotilla-Sanchez, and J. Kim are with the School of Electrical Engineering & Computer Science, Oregon State University, Corvallis, OR, 97331 USA e-mail: {lassettc,ecs,kimjinsu}@oregonstate.edu

similar fashion to successful techniques applied to other power system problems as seen in the research literature. In this paper we propose a machine learning algorithm, specifically a Support Vector Machine, to predict safe times to reconnect a portion of a grid. The Support Vector Machines allow one to build a classifier predicated upon training data by determining a linear separator in a specific feature dimension [13]. As seen in [14] we can create a knowledge base consisting of training and testing data using an appropriate power system model and simulator. Diversity of data points in the knowledge base can be achieved by incorporating load changes allowing multiple operating points [14], [15].

In the proposed machine learning approach, PMU measurements are used as input features that will be used by a learning algorithm to predict which class the features belong to, either stable or unstable reconnection. As of now, PMUs are not as prevalent in the system to assume full state observability in real time, thus it is important to take into consideration limited PMUs when implementing techniques [16]. This paper borrows the concept of electrical distance which suggests voltage changes propagate adhering to closeness of buses [17], [18]. As a result, without getting into the PMU placement optimization problem, this paper assumes that PMUs were located nearby the PCCs.

The contribution of this paper is to introduce a classifier for determining the stability of islands that will be robust in terms of large sub-networks. Current work focuses on small microgrids that have one point of common coupling; we explore other avenues that allow for limited monitoring and intervention of the system. We account for system dynamics to ensure that our classifier will function properly in face of transients. The scalability of the proposed method is tested along with cases with little to no information on the current operating point. In conjunction to proposing a dynamic classifier, we hope to add to the ever growing work on intelligent algorithms to move the future power network to a smarter system. It will be desirable for future control schemes to be autonomous and quick to prevent propagating failures and aid in a self healing network. Lastly we call to attention the need to use larger test cases to prove control techniques. Protective measures may be necessary on large networks to mimic real-life grid behavior as small perturbations may lead to large cascading failures not caught by standard simulations.

The remainder of this paper is organized as follows. Section II gives a brief background of machine learning techniques. Section III covers the methodology to create a power system classifier. Section IV discusses results from experiments with the proposed algorithm. Section V provides the conclusions.

II. Support Vector Machines

We propose to leverage a Support Vector Machine (SVM) to predict stable reconnection timings of a microgrid based on real-time PMU measurements. Conceptually, the SVMs transform an input feature vector into a higher-dimensional space and applies a linear classification rule to predict its class label [19]. In this section, we present the formulation of our learning problem and the preliminaries describing the SVM.

In our context, real-time measurements collected from PMUs form an input vector. The input vector is associated with a binary class label, either 1 or -1, depending on whether reconnection of the microgrid at the current time would lead to a stable operating point or an unstable point, respectively. By using the SVM framework, we aim to build and learn a classifier that maps input vectors to true class labels with high probability. The learned classifier can be used in practice to predict the consequence of a reconnection when certain PMU measurements are observed.

In order to learn a classifier, we need training data consisting of a number of input vectors $x_1, ..., x_n$, and their associated class labels $y_1, ..., y_n$. The methodology to obtain the training data will be explained in Section III. Given a set of training data, the SVM uses a basis function, denoted by $\phi(\cdot)$, to map input vectors into a higher-dimensional space in order to enhance linear separability. The SVM takes these feature vectors as inputs with their corresponding labels and is trained with the information. Specifically, a separating affine hyperplane is obtained by solving the following primal problem:

$$\min_{w,b,\zeta} \frac{1}{2} w^T w + C \sum_{i=1}^{n} \zeta_i \tag{1}$$

subject to

$$y_i(w^T \phi(x_i) + b) \geq 1 - \zeta_i, \quad \zeta_i \geq 0, \ i = 1, 2, ..., n \tag{2}$$

where the regularization term with the parameter C penalizes the training data points that are on the wrong side of the margin. The solutions w^* and b^* to the above optimization define the SVM classifier as follows:

$$f(x) = \text{sign}[(w^{*T} \phi(x) + b^*)] \tag{3}$$

where the offset $b*$ is derived from the dual solutions [19].

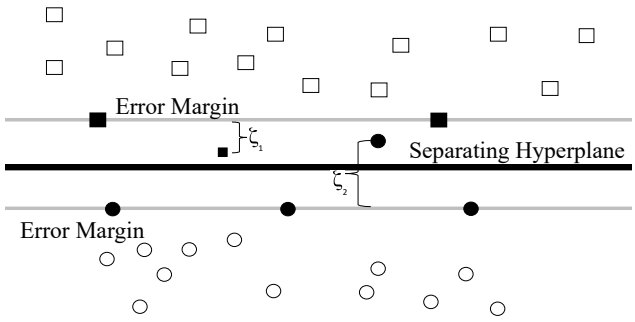

Fig. 1. Example representation of decision and error boundaries for a Support Vector Machine

The example in Figure 1 depicts a classifier built for prediction of two classes. In this example, the squares represent one class and the circles the other. The separating hyperplane is found by solving the optimization problem (1), with error margins existing for each class. A solution may not always

have classes completely separated; the penalty will be associated to the distance past the error margin, ζ_i, and the weight, C.

In the case that the dimension of $\phi(x_i)$ is significantly higher than that of x_i, solving the dual of (1) can lead to an alternative expression of the classifier that is substantially easier to compute. The dual of (1) is:

$$\min_{\alpha} \frac{1}{2}\alpha^T Q\alpha - e^T\alpha \tag{4}$$

subject to

$$y^T\alpha = 0, \quad 0 \leq \alpha_i \leq C, i = 1, 2, ..., n \tag{5}$$

where α_i denotes the Lagrangian multiplier for the ith constraint of (1), and e denotes a vector of all ones. In the dual formulation, the basis function $\phi(\cdot)$ is integrated into the matrix Q by the use of a kernel function $K(x_i, x_j) \triangleq \phi(x_i)^T\phi(x_j)$. Specifically, the (i, j) entry of Q is equivalent to $y_i y_j K(x_i, x_j)$. Many kernels exist, but the most relevant one used in this paper is the Radial Basis Function (RBF), or Gaussian, kernel shown below:

$$K(x_i, x_j) = e^{(-\gamma|x_i - x_j|^2)} \tag{6}$$

where γ is the hyperparameter to be optimized via cross-validation. The solutions of the dual problem provide an alternative expression of the classifier (3):

$$f(x) = \sum_{i=1}^{N} \text{sign}(\alpha_i y_i K(x, x_i) + b) \tag{7}$$

Using the above expression has computational advantages over the use of (3), because $K(x, x_i)$ is in general easier to compute than $w^{*T}\phi(x_i)$. This is true for kernels with the dimension of $\phi(x)$ being significantly larger than x such as the RBF kernel. Further, the majority of weights, α_i, will be zero; only the support vectors will have nonzero weights.

III. Training the SVM using a Dynamic Simulator

In this section, we present the machine learning framework for predicting stable reconnection timings of a microgrid as well as the detailed procedure to train the classifier with a power system dynamic simulator. As suggested earlier, we train the SVM to predict the stability of reconnection for a microgrid when certain PMU measurements are observed. In order to train the SVM, we need to first acquire a set of training examples, each of which is a pair of an input vector (i.e., a vector of PMU measurements) and the true class label (i.e., stable or unstable connection of the microgrid when the measurements are observed). Unfortunately, it is difficult in practice to obtain sufficient training data from realistically sized power systems as obtaining a pair requires disconnecting and reconnecting the microgrid. Thus, we resort to leveraging a power system dynamic simulator to create training data by running a variety of scenarios for the target system.

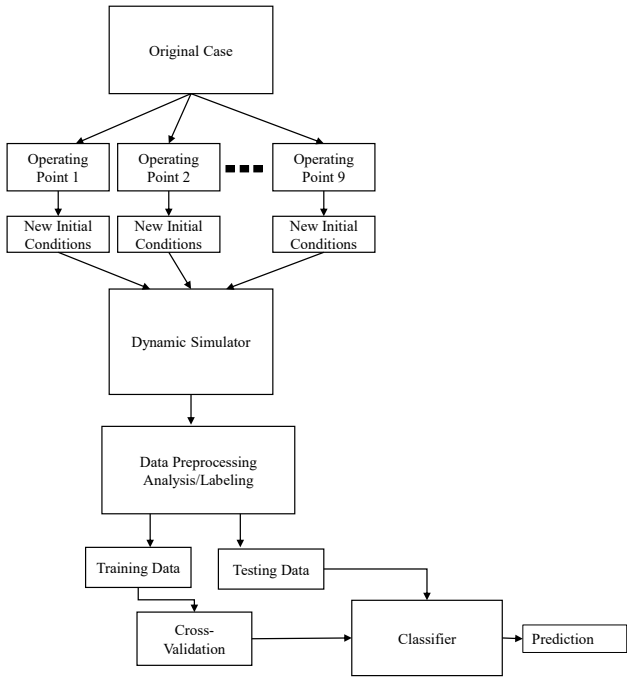

Fig. 2. High level overview of the process to create a classifier

A. Overview

Figure 2 illustrates the algorithm that we follow for the experiments in this paper. We chose the 73-bus version of the IEEE Reliability Test System (RTS-96) [20] and the 2383-bus version of the Poland Test Case to implement our algorithm as they are well tested in the community [21]. The RTS-96 provides a convenient topology to implement and test islanding, whereas Poland serves as a larger network to more closely model a practical system. For the RTS-96 case we used the procedure described below to create several operating points. For the Poland test case we used a modified winter peak snapshot to ensure diverse data could be gathered during the creation of different initial conditions.

We began with a specific network and created different operating points by uniformly changing load locations throughout the network. Loads were also uniformly scaled at random when building these new operating points. We then simulate the dynamics of the system with Siemens PTI PSS/e and perform the islanding and reconnection scenarios. Upon completion of simulations, bus voltages and angles before the reconnection of islands are used as features and the outcome of the case (stable or unstable) are used to label the set. The raw data produced are separated into training and testing sets in which cross-validation is performed to build an adequate classifier.

B. Diversifying Operating Points

It is important to take into account test cases that can reproduce various operating points depending upon, for example, time of the day, day of the week, or season [22]. In this way, the classifier will be useful for a diverse set of network states. We

created different operating points by shuffling and scaling loads at random throughout the system. Upon obtaining the new demand distribution, we ran a steady state solution of the case and considered it stable and usable if the voltage magnitude set was between 0.9 p.u. and 1.1 p.u. For each operating point we created different initial conditions by changing active and reactive loading on each bus, according to Eqs. (8) and (9):

$$P_{\text{new}} = P_{\text{old}} + \theta P_{\text{old}}, \quad \theta \sim \ U(-a, b) \tag{8}$$

$$Q_{\text{new}} = Q_{\text{old}} + \gamma Q_{\text{old}}, \quad \gamma \sim \ U(-a, b) \tag{9}$$

where P_{new} and P_{old} denote the new system active power and original system active power, respectively; Q_{new} and Q_{old} denote the new system reactive power and original system reactive power respectively. For scaling, θ and γ are independent and identically distributed random variables that are uniformly distributed in $[-a, b]$.

C. Dynamic Simulation

We are interested in the interaction between the sub-network and main grid upon reconnection. In order to observe the main reconnection mechanisms, we simulate the power system dynamics with a time-domain simulator software (Siemens PTI PSS/e) along with a custom built command line interface (Python API[1]). We first used a research-grade dynamic simulator alongside PSS/e to cross-validate and tune the dynamic machine models [23], [24]. The dynamic models selected consist of salient machines for the generators, IEEE Type 1 exciters, and IEEE Type 2 governors. We initiate each simulation run in PSS/e with a flat start check in order to ensure the dynamic models do not alter the steady state solution and also that no protective elements are operating during the steady state. We added relay models and protection schemes to our test cases, including overcurrent, undervoltage, and underfrequency relays. The overcurrent relays are set up using the line limit standard data that come with the selected test cases. We configured load-shedding, line-tripping, and generator disconnection actions for undervoltage and underfrequency situations. During the dynamic simulation we monitor bus voltages, angles, and frequencies.

For each initial condition obtained for a given operating point of the original test case we run a dynamic simulation. After the initialization period we proceed to island a predefined portion of the test case in which the two isolated systems run independently for a certain amount of time. The sub-network is then reconnected with the main grid and continues to run until the end of our simulation time.

D. Data Preprocessing Analysis and Labeling

After completion of dynamic simulations we proceed to formulate this problem in terms of machine learning. In order to leverage SVMs we need feature vectors and their associated labels. As stated earlier we create different operating points for our initial test cases, we then create new initial conditions for each operating point for diversity. Each initial condition case will represent a single feature vector along with a single label. The features for each case are represented by the bus voltages and angles observed at the time point before reconnection. Angles were unwrapped to the first turn, between -180 and 180 degrees. We assume that the PMU set is fixed for clarity.

The labels in these experiments represent whether the case became stable or unstable upon reconnection of the sub-network to the main grid. Labeling was done based on the PSS/e convergence monitor which would alert the Python interface if the network did not converge at any point in time. If the API observes the 'network not converged' message, we assume immediately that the PSS/e was unable to solve the differential-algebraic system of equations and label the case unstable. We added additional convergence rules during labeling which allowed more cases to be labeled unstable if voltage collapses, there are very large oscillations, divergence or intolerable frequency spikes occurred. If the case satisfied the rules of stability we provided, it was labeled as stable. We store all case data in the form of their feature vector and label for each operating point. We split the full dataset into two subsets; one representing the training set to create the classifier, and the other one to test the accuracy of the classifier.

E. Classifier

Given the prepared training and testing sets, the next step is to define and build the classifier. As stated earlier, it may be necessary to remap the features to another dimension in which classification is easier, this leads us to choose from different kernels and hyperparameters. SVM is very sensitive to the kernel and hyperparameters chosen, thus it is important to setup the classifier in a way that maximizes our prediction accuracy.

In order to find optimal kernel and hyperparameters, we used k-fold cross validation. We keep track of accuracies and then repeat the entire procedure with a new kernel and hyperparameter setup. Upon completion, we choose the kernel and hyperparameters setup that yielded the highest accuracy.

The next step is to train the classifier with the entire set of training data available. Upon completion of training, the classifier is able to make predictions of classes based on an input feature vector. Specifically, the classifier predicts whether the system it has been trained on will be stable or unstable if it were to reconnect at the given time. We made use of the Python library *scikit-learn*, which includes implementations of machine learning algorithms such as SVM.

IV. Results

In this section, we present the performance of the proposed method for predicting stability of microgrid reconnection. For evaluation, we used the RTS-96 test case and the Poland case. As stated previously, the proposed classifier can account for multiple PCCs in a network. For example, due to the choice of islanding Zone 3 in the RTS-96, we consider the two PCCs shown in Figure 3.

[1]Application Program Interface

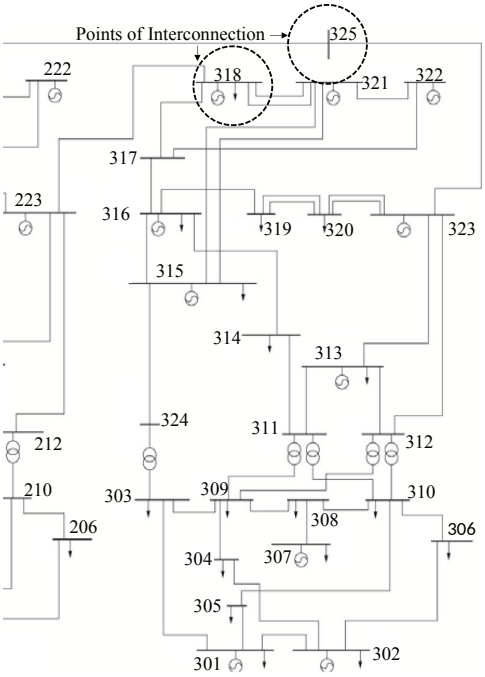

Fig. 3. Points of interconnection in the RTS-96 case.

TABLE I. CLASSIFIER SETUP AFTER CROSS-VALIDATION

Operating point	Kernel	γ	C
1	RBF	0.000001	100
2	RBF	0.0001	10
3	RBF	0.000001	10
4	RBF	0.000001	10
5	RBF	0.00001	1
6	RBF	0.0001	10
7	RBF	0.00001	1
8	RBF	0.000001	10
9	RBF	0.00001	0.1

TABLE II. ACCURACIES FOR RTS-96 OPERATING POINTS INDEPENDENTLY TRAINED

Operating point	Class 1 accuracy [%]	Class 0 accuracy [%]
1	97.8	100
2	80	99.2
3	90.7	97.1
4	97	80
5	84.7	89.6
6	91.3	85.9
7	89.5	86.0
8	96.7	90.6
9	90.6	81.3
Average	90.9	90

A. RTS-96

For the RTS-96 case we created nine different operating points and gathered 400 different initial conditions for each. The RTS-96 case is made up of three sub-networks that are mostly identical to one another, and we chose to island Zone 3 which contained bus numbers in the 300s. The intentional islanding occurred five seconds into the simulation, the reconnection event occurred at 45 seconds, and we terminated the simulation at 120 seconds. We did not implement protection schemes for this baseline scenario.

We began by creating a classifier for each operating point and observed the accuracy attained on each class. To ensure our classifier can predict on truly unknown cases, we implement cross-validation to choose the hyperparameters discussed previously for a particular classifier. For each operating point we chose 100 cases of class stable and 100 cases of class unstable to train the classifier. We applied 10 fold cross validation, thus we created 10 sets of 20 cases from the training set and performed cross-validation with a linear, polynomial, and radial based function kernel (RBF). From these we observed the best performance was achieved with the RBF kernel along with a specific set of hyperparameters. Some operating points had differing hyperparameters when their classifiers were built. As such, Table I shows the selected hyperparameters for each operating point.

We observed that training and testing on individual operating points yields results that suggest some are easier to predict than others. The worst case operating point can predict unstable cases with an accuracy of 80%, as seen in Table II, however most other operating points can make predictions at a much higher accuracy. In Table II, Class 0 represents unstable reconnections and Class 1 represents stable reconnections.

We also investigated a generalized classifier that assumes an operator would not have immediate access to detailed knowledge of the current operating point of the system. With this assumption, we create a universal classifier by combining all nine operating points, and training with 100 stable and 100 unstable cases from every operating point. The reason for training with the same number of stable and unstable cases ensures we do not create a classifier that could potentially be skewed based on the priori of the class distributions in the total examples obtained. Similarly we use 200 cases from each operating point to ensure no operating point dominates the classifier during training.

TABLE III. ACCURACIES FOR RTS-96 OPERATING POINTS JOINTLY TRAINED

Operating point	Class 1 accuracy [%]	Class 0 accuracy [%]
1	86.8	100
2	97	72
3	79.2	99.4
4	90.1	82.9
5	89.4	88.7
6	100	78
7	91.2	88.8
8	95.6	92.5
9	93	74
Average	91.4	86.3

We performed the aforementioned cross-validation technique and obtained the best classifier, which is an RBF kernel with a γ value of 0.00001 and a C value of 1. We tested on the remaining cases of each operating point, shown in

Table III. We kept the operating points separate to observe how well the combined classifier does on each particular case and combined the average accuracies obtained to assert the generalized accuracy of the classifier. The accuracy of the classifier is based upon the selection of a case at random from each operating point disregarding the priori of both the distribution of cases throughout the operating points as well as the priori of the classes. It is fairly intuitive why we chose to ignore the distribution of stable and unstable cases during data acquisition. If our operating point is at a point in which most cases with differing initial conditions are stable when reconnecting the islands, and we choose to use this information during training, it could result in favoring the prediction of stable cases. With so many possible initial conditions that can be obtained for each operating point, it is safer to disregard the priori even if it degrades our accuracy slightly.

1) Inference with a small subset of PMUs: We investigated the performance of the proposed method when only a small subset of PMUs are used for classification. It turned out that using a smaller subset of PMUs does not substantially degrade performance if the subset is properly chosen. Among the assumed PMU locations, we selected a PMU to be allowed in the trusted subset only if they were immediately adjacent to a PCC in the network. As a result we can choose a handful of desired PMUs to be used. The full set of PMUs considered for RTS-96 were at buses: 118, 121, 218, 221, 223, 318, 321, 323, 325. Out of these desired PMUs, for this experiment we only selected either two or three to be secure, then we trained and tested on the smaller subset. Table IV illustrates the results of this experiment, whereby Class 1 represents a stable reconnection and Class 0 represents an unstable reconnection.

TABLE IV. ACCURACIES FOR RTS-96 OPERATING POINTS WITH SUBSETS OF TRUSTED PMUS

PMU location [bus number]	Class 1 accuracy [%]	Class 0 accuracy [%]
118, 318	92.7	87.6
118, 321	92.8	87.6
121, 318	92.4	87.5
118, 121	90.1	85.6
323, 325	92.2	86.8
218, 321, 325	93.4	87.2
221, 223, 323	94.1	86.6
121, 218, 318	93.2	87.3
118, 121, 218	90.2	86.0
318, 323, 325	94.3	86.4

The main reason for obtaining better results with limited PMUs in some test cases is due to the exclusion of PMUs that are either adding noise to the classifier or not providing relevant information. A higher number of features leads to the need for more training data to create an adequate classifier. If we use PMUs that do not provide useful information, building the classifier becomes difficult with limited training data. We observe that it may not be feasible to produce large quantities of training data which can lead to better results from subsets of PMUs rather than the entire set. This is shown in randomly chosen subsets in Table IV for RTS-96 as well as in the following section for the Poland case.

The above results suggest that the proposed method can be adjusted to be resilient to potential cyber attacks that may manipulate part of PMU data. In the event that the integrity of PMU measurement data is not fully guaranteed due to cyber threats [25], we cannot rely on the classifier processing the full set of PMU measurements. To effectively handle such a case, we can prioritize protection of a certain small subset of PMUs such that the integrity of their measurements can be strongly guaranteed even in the presence of cyber adversaries. Our results imply that if the trusted subset is properly chosen, the classifier can perform with high accuracy based on the trusted PMU measurements.

B. Poland Network

Due to the size of the Poland Network, for this experiment we limited ourselves to use one baseline operating point (with uniformly distributed variations of load) in which we tested our algorithm on. We incorporated a protective scheme by adding overcurrent relays on each transmission line, as well as undervoltage and underfrequency relays on each bus. We allowed relay operation to trip lines, shed load, or disconnect generators. The overcurrent relays were set based upon the transmission line limits from the original test case. Table V provides an overview on the relay configuration.

TABLE V. OVERCURRENT RELAY CONFIGURATION

Point	Pickup [%]	Trip time [sec.]
1	100	5
2	125	0.2
3	137.5	0.15
4	150	0.1

Underfrequency and undervoltage relays were used for bus and generator monitoring and protection. Setting the voltage thresholds is straightforward given the baseline variability of voltages for each bus. Frequency variability is more challenging to set up without obtaining more information from the operation of a large network. Thus, we grouped buses with similar frequency response and introduced different frequency threshold points throughout the system. As a result, load shedding and generator tripping due to underfrequency events allowed for heterogeneous disconnection, generally a more accurate depiction of system survival in a real case. Synthesized time-dial points for underfrequency bus relays were setup as shown in Table VI, depicted by rows (LS). For generator relays, a random value ($y = \{1, 2, 3, 4\}$) was chosen and scaled for the time-dial points shown in Table VI, depicted by rows (GR).

Since the Poland test case is divided by default into five zones, we solved the steady state of the case when islanding certain zones. Zone 5 was a good candidate for intentional islanding due to a low mismatch for generation and demand, as well a voltages within acceptable operating limits, thus it was selected to be the sub-network of interest in this experiment. During the dynamic simulations we islanded the sub-network at 2 seconds. We reconnected the sub-network with the rest of the grid at 25 seconds and terminated the simulation at 55

TABLE VI. UNDERVOLTAGE/UNDERFREQUENCY LOAD SHEDDING (LS) AND UNDER/OVER FREQUENCY GENERATOR (GR) RELAY CONFIGURATIONS

Point	Pickup volt. [p.u.]	Trip [sec.]	Pickup freq. [Hz.]	Trip [sec.]
LS 1	0.92	5	49.5	5, 4, 3, 2
LS 2	0.88	0.5	49	2, 1.5, 1, 0.5
LS 3	0.75	0.2	48.5	1, 0.75, 0.5, 0.25
GR 1	-	-	48.5, 51.5	y
GR 2	-	-	47.5, 52.5	$y/2$
GR 3	-	-	46, 54	$y/4$

seconds. Unlike the RTS-96 experiment, we did not assume full PMU coverage of a large scale network to begin with. We only allowed a PMU in the available set if it is immediately attached to the interconnection between the sub-network and the main grid. We were left with 36 available buses in the Poland network to build a feature vector. As we stated earlier in the algorithm description, the next step was to create labels based on the convergence of the case. Figures 4 and 5 illustrate labeling examples for stable and unstable cases, respectively.

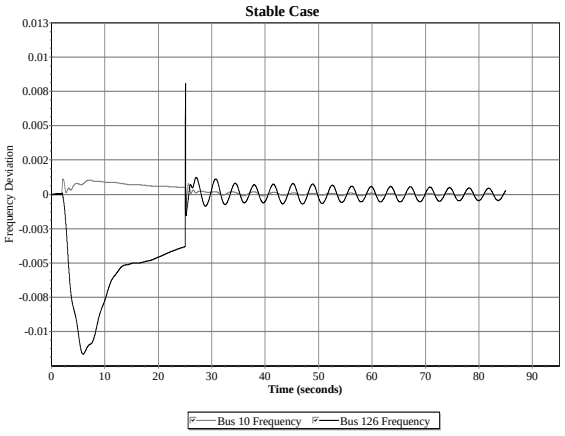

Fig. 4. Stable reconnection of a Poland network scenario

Figures 4 and 5 depict frequencies of two buses on either side of an interconnection point. One can observe that case labeled as stable case exhibits a reconnect where the frequency signals converge to a common operating state. The unstable case shows the frequency of Bus 126 spike and immediately flat-line representing a bus trip. As described in the methodology section, if the network did not converge, it would have immediately been labeled unstable. The rules of stability in the Poland case additionally enforced that at least 2370 of the 2383 buses in the case were in service after reconnection of the island.

We created 550 different initial condition cases and then trained with 100 stable and 100 unstable cases. We used the cross-validation method to determine the best kernel and hyperparameters using only the training data. Upon completion of 10 fold cross-validation the RBF kernel was selected with a γ value of 0.01 and a regularization coefficient of 10. It is

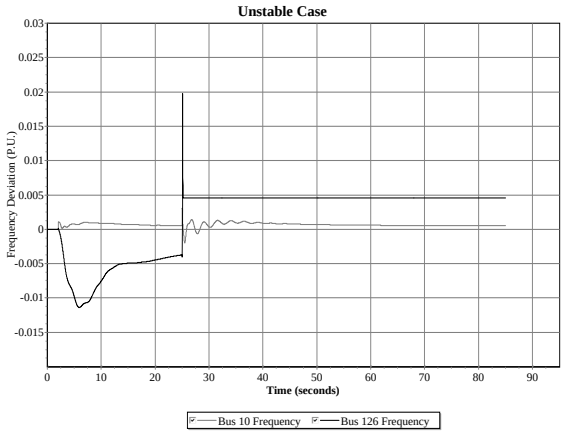

Fig. 5. Unstable reconnection of a Poland network scenario

important to note that formal cross-validation on the Poland test case yielded the aforementioned setup. However we also observed that a γ value of 0.0 and regularization coefficient of 10 were fairly close in accuracy during cross-validation. An RBF kernel with a γ value of 0.0 can be seen as a linear mapping. The former setup was reported in the results as it was the most recurring setup from a large amount of cross-validation trials. We trained the classifier with the newly found kernel, hyperparameters and full training set. We tested on the remaining cases with our classifier and recorded the accuracies obtained.

TABLE VII. ACCURACIES FOR BASELINE POLAND NETWORK

	Class 1 accuracy [%]	Class 0 accuracy [%]
Poland network	90.2	98.3

TABLE VIII. ACCURACIES FOR POLAND NETWORK WITH SUBSETS OF TRUSTED PMUS

PMU location [bus number]	Class 1 accuracy [%]	Class 0 accuracy [%]
165, 1883, 2333	93.1	98.3
166, 2226, 2278	93.1	97.8
125, 186, 2124	91.4	96.6
174, 186, 1883	90.8	97.1
335, 2248, 2331	91.4	96.6

The resulting accuracies of the predictor in the Poland experiment can be seen in Table VII. These results suggest that the proposed classifier is well suited when scaling up to larger testing systems, a desirable behavior to tackle real-sized power system problems. As stated earlier for the smaller test case experiments, we also investigate the accuracy of the classifier for a scenario when the system is compromised. As a response, our classifier makes use of a trusted set of PMUs and makes predictions based on their measurements. A variety of subsets from the available PMU full set make up our possible trusted scenarios, as shown in Table VIII.

In the larger Poland case it seems more prevalent that decreasing the amount of features can lead to an even better

performing classifier. The adoption of this control technique would bring into question whether a utility could provide enough training data, specifically the number of training examples, for the classifier. If limited training data is provided, the usage of optimal PMUs instead of the entire available set could yield better accuracies. Indeed it is always interesting to observe that less amount of information give better results, and it is explained in this case by considering a high dimensional feature space it can readily be understood that it becomes much more difficult to create an accurate linear separator. Utilities with the ability to archive and make available relatively large amounts of training data could still make use of a larger feature set, if available, and potentially observe higher accuracies with respect to the quantity of training examples provided in these experiments.

V. Conclusion

This paper presents a machine learning approach for the prediction of stable reconnections of a power system subnetwork. The proposed approach leverages a power system dynamics simulator to generate synthetic, yet realistic in terms of size, training examples that are subsequently employed to train a classifier. The interactions between power system dynamics and protection mechanisms are complex, and the exact derivation of an optimal control strategy is not always feasible. However, as demonstrated in this paper, a machine learning approach can be useful to capture many unintuitive behaviors and make predictions in real-time based on PMU measurements. The classifier was tested on a variety of cases and operating points to ensure diversity. Accuracies of approximately 90% were observed throughout most conditions when making dynamic predictions of a given network.

Acknowledgment

This material is based upon work supported by the Department of Energy under Award Number de-oe0000780.

References

[1] J. Chadwick, "How a smarter grid could have prevented the 2003 U.S. cascading blackout," in *Power and Energy Conference at Illinois (PECI), 2013 IEEE*, Feb 2013, pp. 65–71.

[2] A. Phadke, "Synchronized phasor measurements in power systems," *IEEE Computer Applications in Power*, vol. 6, no. 2, pp. 10–15, 1993.

[3] J. Burnett, R.O., M. Butts, and P. Sterlina, "Power system applications for phasor measurement units," *IEEE Computer Applications in Power*, vol. 7, no. 1, pp. 8–13, 1994.

[4] T. Cease and B. Feldhaus, "Real-time monitoring of the TVA power system," *IEEE Computer Applications in Power*, vol. 7, no. 3, pp. 47–51, July 1994.

[5] A. Phadke, "Synchronized phasor measurements-a historical overview," in *Transmission and Distribution Conference and Exhibition 2002: Asia Pacific. IEEE/PES*, vol. 1, Oct 2002, pp. 476–479.

[6] F. Tang, J. M. Guerrero, J. C. Vasquez, D. Wu, and L. Meng, "Distributed active synchronization strategy for microgrid seamless reconnection to the grid under unbalance and harmonic distortion," *IEEE Transactions on Smart Grid*, vol. 6, no. 6, pp. 2757–2769, 2015.

[7] S. K. Khadem, M. Basu, and M. F. Conlon, "Intelligent islanding and seamless reconnection technique for microgrid with upqc," *IEEE Journal of Emerging and Selected Topics in Power Electronics*, vol. 3, no. 2, pp. 483–492, June 2015.

[8] T. M. L. Assis and G. N. Taranto, "Automatic reconnection from intentional islanding based on remote sensing of voltage and frequency signals," *IEEE Transactions on Smart Grid*, vol. 3, no. 4, pp. 1877–1884, Dec 2012.

[9] E. Alegria, T. Brown, E. Minear, and R. H. Lasseter, "Certs microgrid demonstration with large-scale energy storage and renewable generation," *IEEE Transactions on Smart Grid*, vol. 5, no. 2, pp. 937–943, March 2014.

[10] M. A. Sofla and R. King, "Control method for multi-microgrid systems in smart grid environmentstability, optimization and smart demand participation," *IEEE PES Innovative Smart Grid Technologies (ISGT)*, pp. 1–5, Jan 2012.

[11] K. Jones, A. Pal, and J. Thorp, "Methodology for performing synchrophasor data conditioning and validation," *IEEE Transactions on Power Systems*, vol. 30, no. 3, pp. 1121–1130, 2015.

[12] S. Tamronglak, S. Horowitz, A. Phadke, and J. Thorp, "Anatomy of power system blackouts: preventive relaying strategies," *IEEE Transactions on Power Delivery*, vol. 11, no. 2, pp. 708–715, 1996.

[13] C. Cortes and V. Vapnik, "Suppor-vector networks," *Machine Learning*, vol. 20, no. 3, pp. 273–297, 1995.

[14] Y. Zhang, T. Li, G. Na, G. Li, and Y. Li, "Optimized extreme learning machine for power system transient stability prediction using synchrophasors," *Mathematical Problems in Engineering*, 2015.

[15] I. Saeh and M.W.Mustafa, "Machine learning classifiers for steady state security evaluation in power system," *International Journal of Computer Science*, vol. 9, no. 2, pp. 262–269, 2012.

[16] M. Zhou, V. Centeno, J. Thorp, and A. Phadke, "An alternative for including phasor measurements in state estimators," *Power Systems, IEEE Transactions on*, vol. 21, no. 4, pp. 1930–1937, Nov 2006.

[17] E. Cotilla-Sanchez, P. Hines, C. Barrows, and S. Blumsack, "Comparing the topological and electrical structure of the north american electric power infrastructure," *Systems Journal, IEEE*, vol. 6, no. 4, pp. 616–626, Dec 2012.

[18] E. Cotilla-Sanchez, P. Hines, C. Barrows, S. Blumsack, and M. Patel, "Multi-attribute partitioning of power networks based on electrical distance," *Power Systems, IEEE Transactions on*, vol. 28, no. 4, pp. 4979–4987, Nov 2013.

[19] J. Bell, *Support Vector Machines*. John Wiley & Sons, Inc, 2014, pp. 139–160. [Online]. Available: http://dx.doi.org/10.1002/9781119183464.ch7

[20] P. Wong, P. Albrecht, R. Allan, R. Billinton, Q. Chen, C. Fong, S. Haddad, W. Li, R. Mukerji, D. Patton, A. Schneider, M. Shahidehpour, and C. Singh, "The IEEE reliability test system-1996," *IEEE Transactions on Power Systems*, vol. 14, no. 3, pp. 1010–1020, 1999.

[21] R. D. Zimmerman, C. E. Murillo-Sanchez, and R. J. Thomas, "Matpower: Steady-state operations, planning, and analysis tools for power systems research and education," *IEEE Transactions on Power Systems*, vol. 26, no. 1, pp. 12–19, Feb 2011.

[22] A. Sankarakrishnan and R. Billinton, "Sequential Monte Carlo simulation for composite power system reliability analysis with time varying loads," *IEEE Transactions on Power Systems*, vol. 10, no. 3, pp. 1540–1545, 1995.

[23] C. Parmer, E. Cotilla-Sanchez, H. K. Thornquist, and P. D. Hines, "Developing a dynamic model of cascading failure for high performance computing using Trilinos," in *Proceedings of the First International Workshop on High Performance Computing, Networking and Analytics for the Power Grid*, ser. HiPCNA-PG '11. ACM, 2011, pp. 25–34. [Online]. Available: http://doi.acm.org/10.1145/2096123.2096131

[24] J. Song, E. Cotilla-Sanchez, G. Ghanavati, and P. D. H. Hines, "Dynamic modeling of cascading failure in power systems," *IEEE Transactions on Power Systems*, vol. 31, no. 3, pp. 2085–2095, 2016.

[25] S. Mousavian, J. Valenzuela, and J. Wang, "A probabilistic risk mitigation model for cyber-attacks to PMU networks," *IEEE Transactions on Power Systems*, vol. 30, no. 1, pp. 156–165, Jan 2015.